Nanoparticle-Aided Characterization of Arterial Endothelial Architecture During Atherosclerosis Progression and Metabolic therapy

Thijs J. Beldman[1,], Tsveta S. Malinova[2,*], Emilie Desclos[3], Anita E. Grootemaat[3], Aresh L.S. Misiak[1], Saskia van der Velden[1], Cindy P.A.A. van Roomen[1], Linda Beckers[1], Henk A. van Veen[3], Przemyslaw M. Krawczyk[4], Ron A. Hoebe[3], Judith Sluimer[5], Annette E. Neele[1], Menno P.J. de Winther[1,6], Nicole N. van der Wel[3], Esther Lutgens[1,6], Willem J.M. Mulder[1,7], Stephan Huveneers[2], Ewelina Kluza[1,#]*

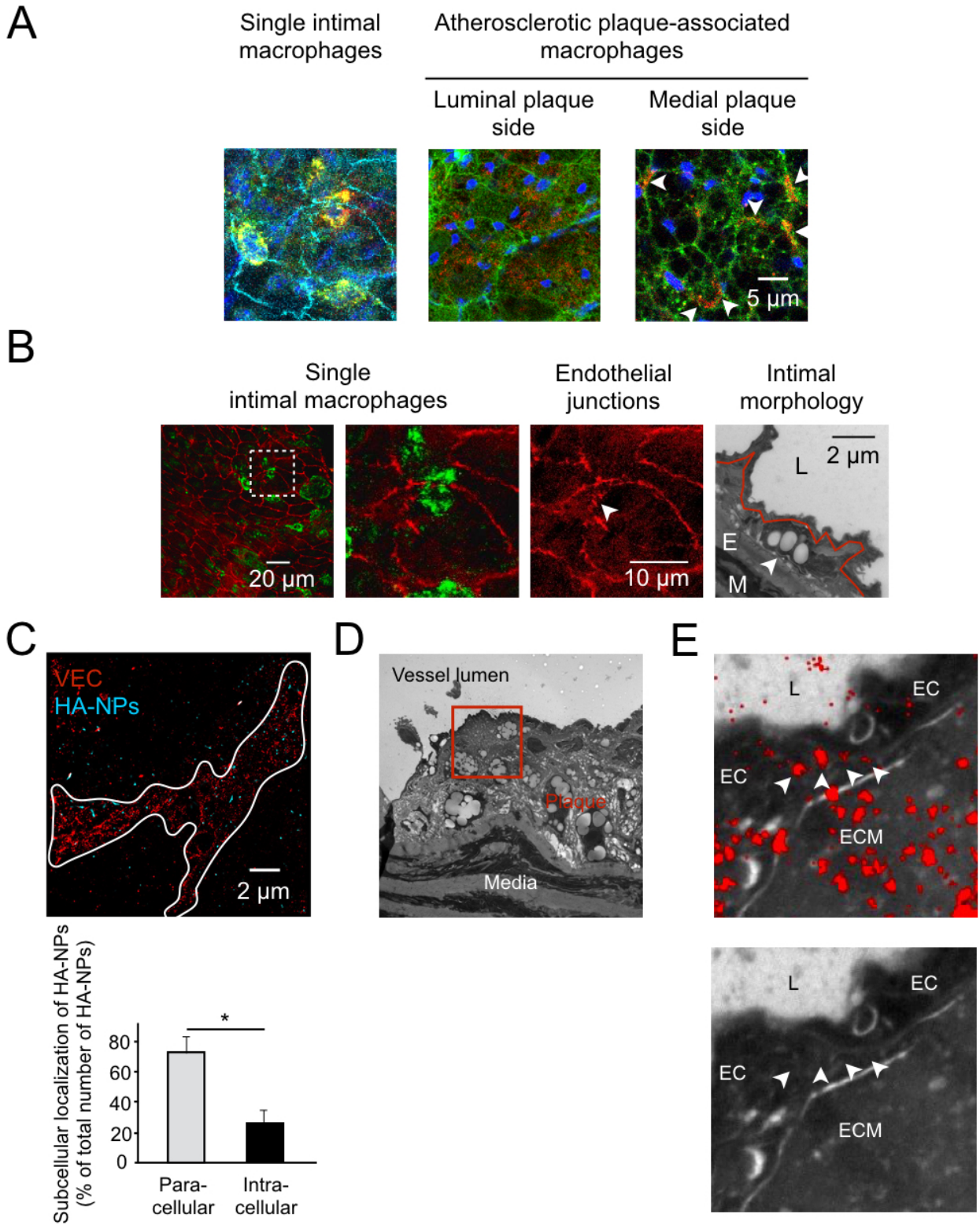

Figure S1 **A**) Overlay images of intimal/plaque-associated macrophages and hyaluronan nanoparticles (HA-NPs), presented in Figure 1D. MAC-3 (green), HA-NPs (red), VEC (cyan blue), DAPI (blue). **B**) In the left, confocal microscopy image displays intimal infiltration of single macrophages. The white frame depicts a region of interest (ROI), which is shown in the following three panels. Macrophages and endothelial junctions were stained with MAC-3 (green) and vascular endothelial cadherin (red), respectively. In the third image, white arrowhead indicates a disrupted endothelial junction. Cy5.5-labeled hyaluronan nanoparticles (HA-NPs), which were administered intravenously 2 h before the mouse sacrifice, are shown in cyan blue (fourth image). In the right, transmission electron microscopy image of a single intimal macrophage (white arrowhead), covered

by thin and highly deformed endothelial layer (hypointense, outlined from medial side with a red line). L: lumen, E: elastin, M: media. **C**) Upper panel displays representative two-color ground state depletion (GSD) microscopy image of the endothelial plaque surface, with a defined VEC-rich (red) cell-cell junction (white ROI). HA-NPs are shown in cyan blue. Lower bar chart compares the percentages of para- and intra-cellular HA-NPs in the atherosclerotic endothelium based on GSD microscopy data (n=13). **D**) Transmission electron microscopy image of a 200 nm-thick section through the atherosclerotic aortic arch. Red ROI depicts the region that was imaged with ground state depletion (GSD) super-resolution microscopy and is shown in **Figure 3C**. **E**) Correlative light and electron microcopy image (upper) displaying HA-NPs (red) in the plaque-covering endothelial layer and the corresponding electron microscopy (EM) image (lower). Notably, the endothelial junctions cannot be clearly identified from EM images because of the section thickness. In all charts, bars represent mean ± SD. Symbol "*" indicates a significant difference at $p<0.05$. In **C**), the data were tested using a two-tailed paired Student's t-test.

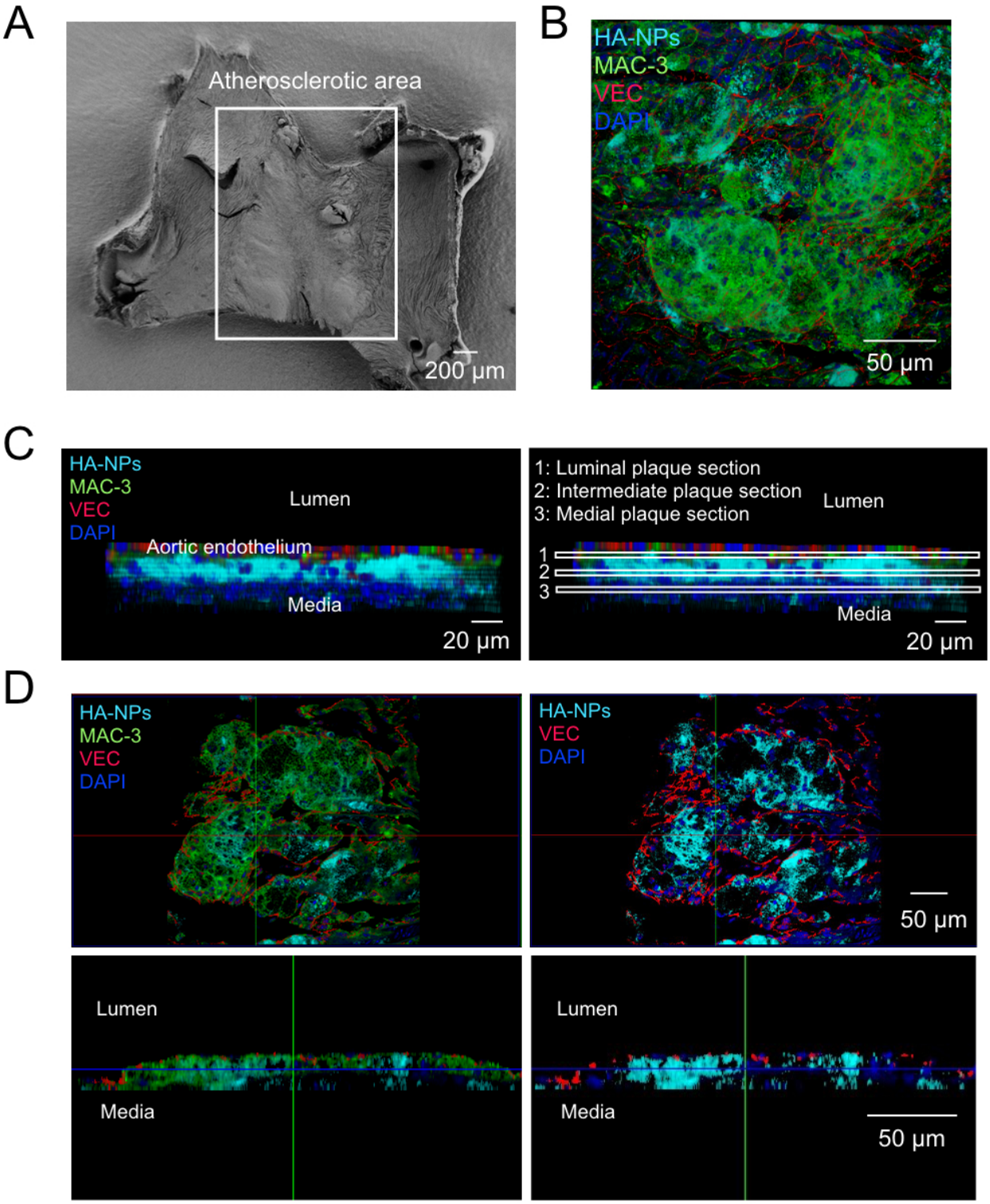

Figure S2 A) Representative *en face* scanning electron microscopy image of an aortic arch sample. The vessel was cut-opened to expose the endothelial surface. White ROI outlines the atherosclerosis-rich area. **B**) Representative 3D visualization of macrophage-rich atherosclerotic foci, oriented according to the imaging plane. Hyaluronan nanoparticles (HA-NPs) are shown in cyan blue, macrophages in green (MAC-3 staining), vascular endothelial cadherin (VEC) in red, and DAPI in blue. The same color-coding is used for other images. **C**) Representative 3D plaque data from the cross-section perspective. Left image shows HA-NP signal localized under atherosclerotic endothelium in the MAC-3-positive areas, but not "invading" the media. Based on the same image, right panel depicts the image sections that were used to demonstrate the heterogeneity of HA-NP intra-plaque distribution in **Figure 1C**. **D**) *En face* (upper panel) and cross-

section (lower panel) images of a plaque showing a heterogeneous distribution of HA-NPs. The location of lower cross-sections is depicted by the red line in upper images.

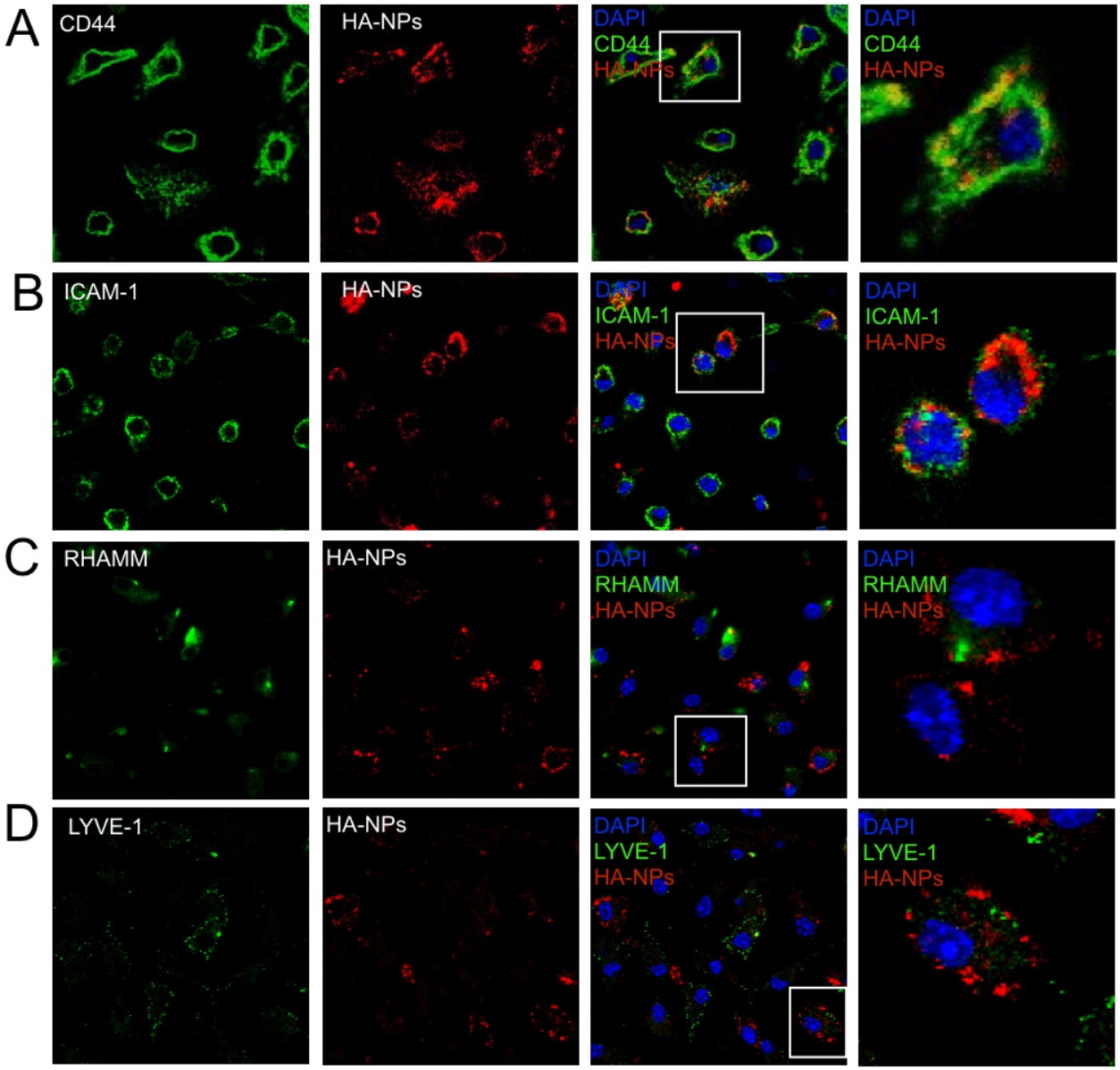

Figure S3 Confocal microscopy images of bone marrow-derived macrophages that were incubated with 50 μg/mL of Cy5.5-HA-NPs (red) for 5 hours at 4 °C. The cells fixed with 4% PFA and stained with either **A**) anti-CD44, **B**) anti-ICAM-1 **C**) anti-RHAMM or **D**) LYVE-1 antibody (all shown in green). Cell nuclei were stained with DAPI (blue in merged images). First and second panel display the receptor staining and HA-NP signal, respectively. Overlay images are shown in the third panel. White ROIs are enlarged in the fourth panel.

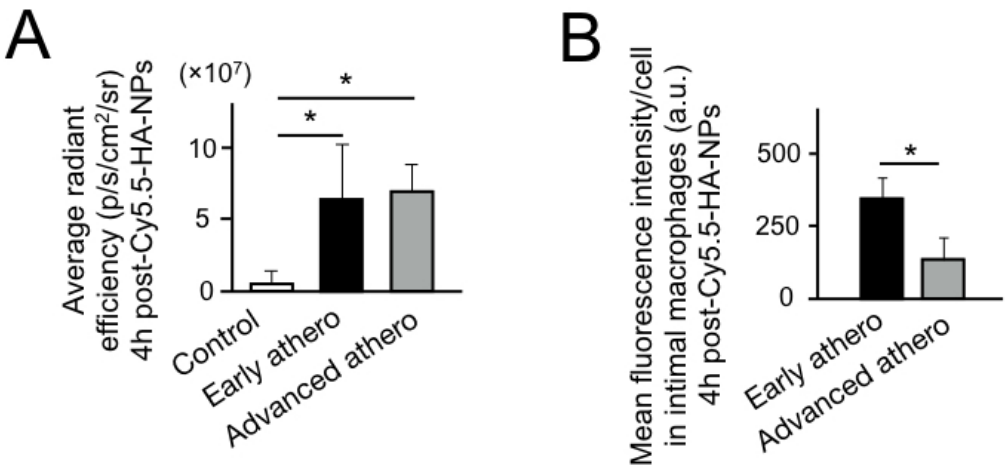

Figure S4 A) Average radiant efficiency acquired by optical imaging in aortic arch of wild-type mice (Control, baseline autofluorescence) and apoE$^{-/-}$ mice after six- (Early athero) or 12-week (Advanced athero) high-fat diet, which were sacrificed and perfused with buffered saline 4h after intravenous administration of Cy5.5-labeled HA-NPs. **B**) Mean fluorescence intensity per cell in plaque-associated macrophages assessed by flow cytometry 4 hours after Cy5.5-HA-NP injection. "*" indicates significant difference at $p<0.05$. In **A**), data was tested with one-way ANOVA with Tukey's post hoc test whereas in **B**), with a student t-test.

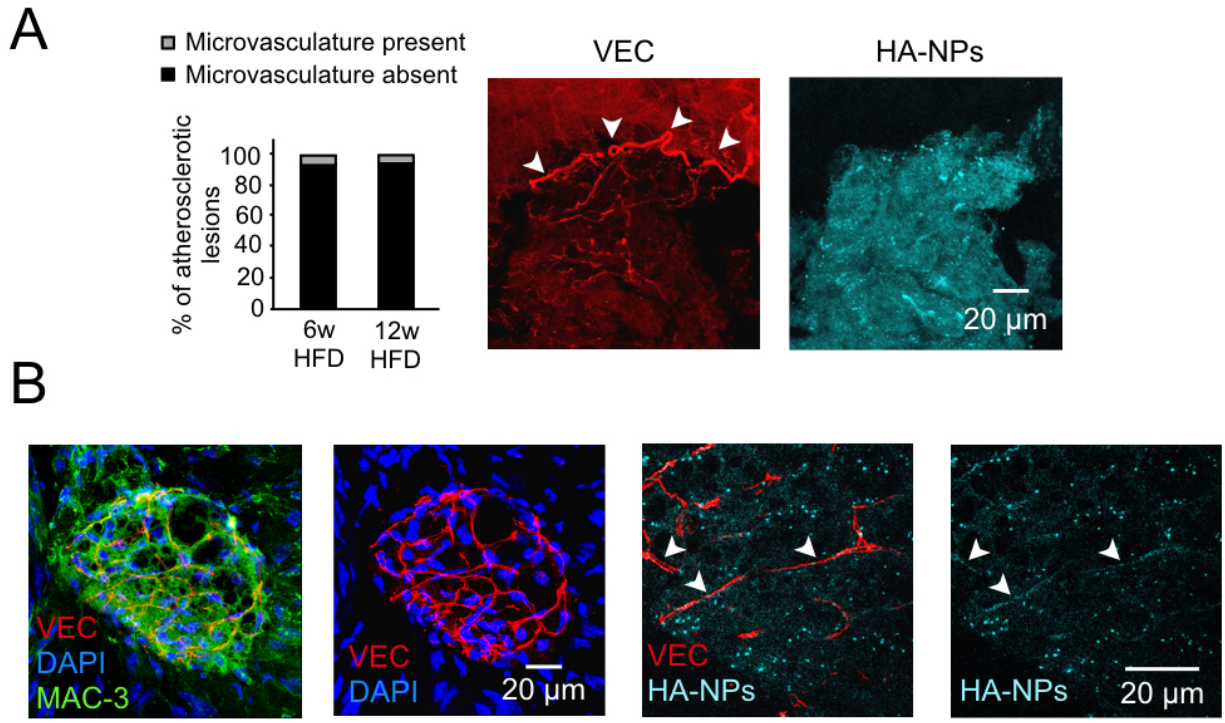

Figure S5 A) The percentage of plaques without (black) and with microvasculature (gray) in early and advanced atherosclerosis mice (left panel). Left panel displays one of few plaques with microvasculature, originating from the luminal endothelium. Images display VEC staining (left, red) and HA-NP fluorescence (right, cyan blue). **B**) Maximum intensity projection of a small plaque displaying extensive microvascular network (first and second image; VEC: red MAC-3: green, DAPI: blue). In third and left image, arrowheads point into microvessels that carry HA-NPs.

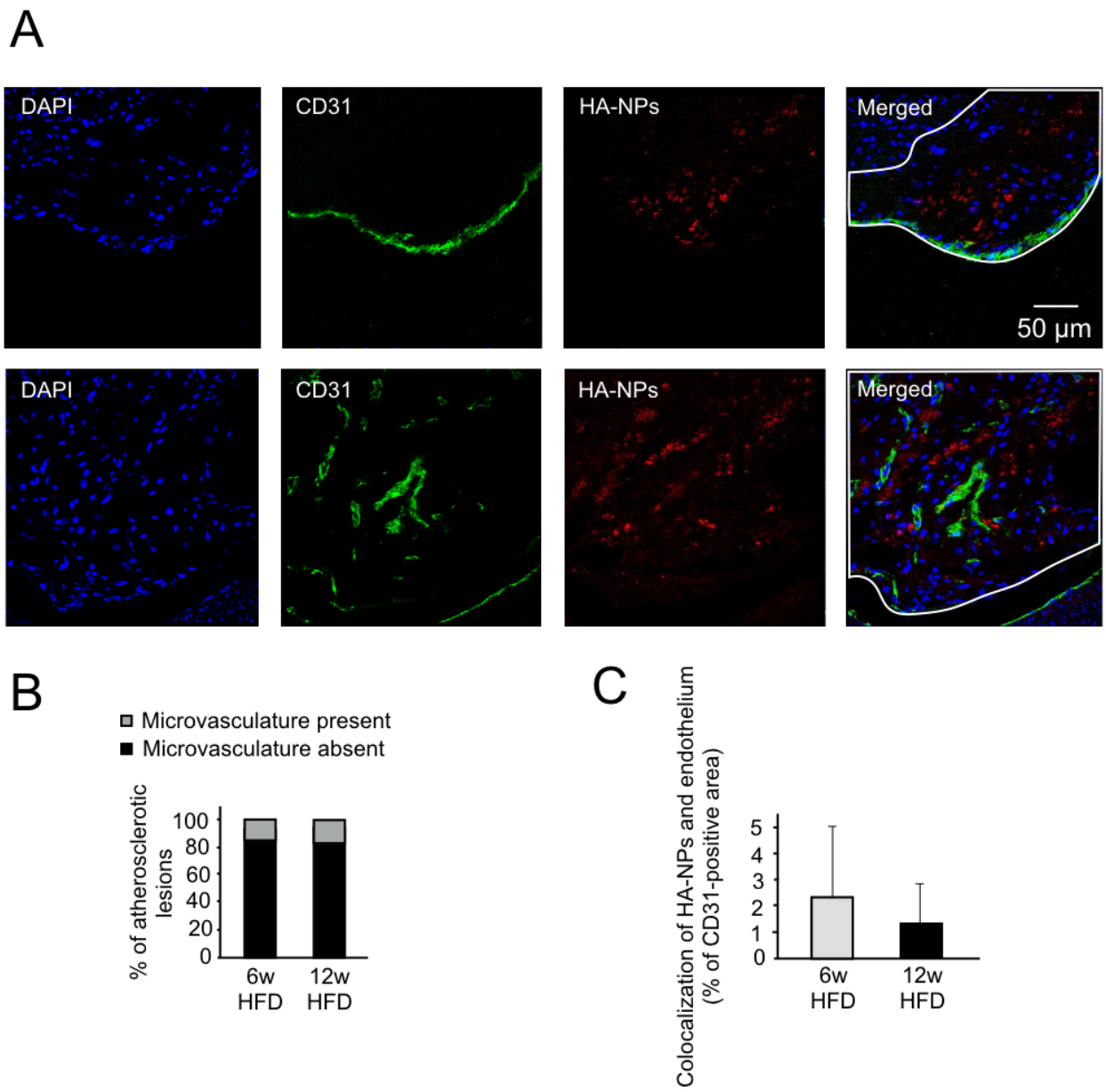

Figure S6 A) Representative confocal microscopy images of aortic arch sections obtained 24 h after administration of HA-NPs in early atherosclerotic mice. HA-NPs (red) are shown in context of CD31-stined macro- (upper panel) and microvascular (lower panel) plaque endothelium (green). HA-NPs efficiently extravasated into to the plaque interior in both the absence and presence of microvasculature. Notably, HA-NPs were not internalized by endothelial cells, but they were located in their proximity. Cell nuclei were stained with DAPI (blue). White lines depict the plaque location, whereas the scale bar shown in the upper right image refers to all other images. **B**) The percentage of plaques without (black) and with microvasculature (gray) in early (6w HFD) and advanced atherosclerosis mice (12w HFD), determined from CD31-stained aortic arch sections (n = 43 and 42, respectively). **C**) The percentage of HA-NP-positive area that colocalized with CD31-stained endothelial cells in aortic plaque sections of early and advanced atherosclerotic mice (n = 43 and 42, respectively). Bars represent mean ± SD.

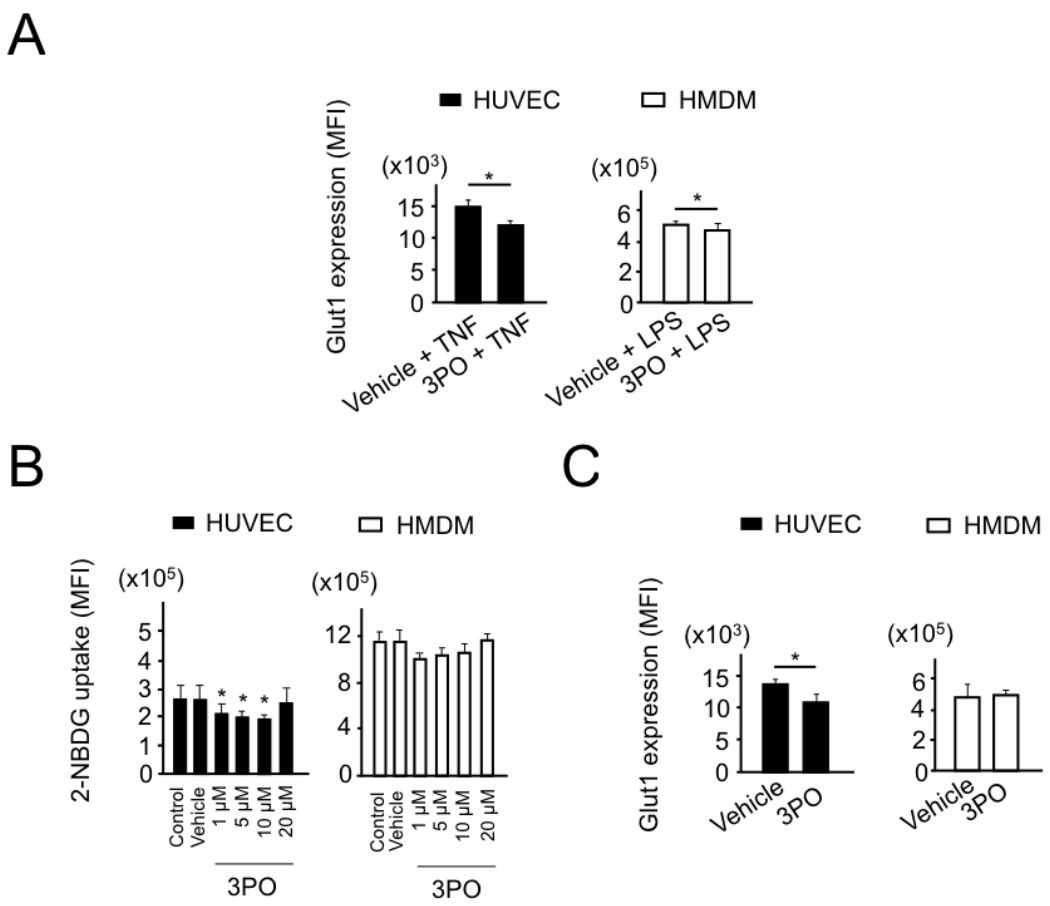

Figure S7 *In vitro* metabolic effects of 3PO in human umbilical vascular endothelial cells (HUVEC) and human monocyte-derived macrophages (HMDM). **A**) Glut1 expression in vehicle- and 3PO-treated HUVEC (left) and HMDM (right), which were co-stimulated for 24 hours with TNF (10 ng/mL) and LPS (100 ng/mL), respectively. **B**) The uptake of 2-NBDG, a fluorescent glucose analogue, in cells that were incubated with either a pure culture medium (Control), 0.03% DMSO (Vehicle), or different concentrations of 3PO, ranging from 1 – 20 μM for 24h. **C**) Glut1 expression in vehicle- and 3PO-treated HUVEC (left) and HMDM (right). "*" indicates significantly lower values compared to the control at $p<0.05$. The multiple group comparison was performed with a one-way ANOVA, followed by a Tukey's *post hoc* test. The Glut1 expression data were analyzed using a two-tailed unpaired Student's t-test.

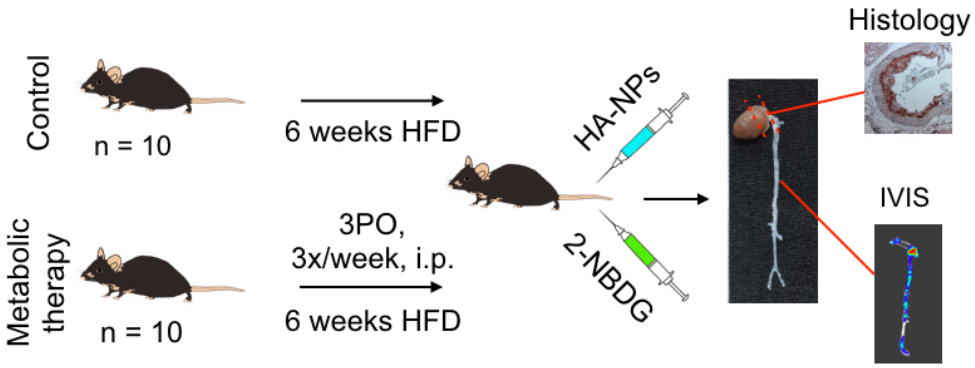

Figure S8 Schematic representation of the experimental setup used to study therapeutic effects of 3PO. *Apoe*$^{-/-}$ mice underwent six-week treatment combined with a high-fat diet (HFD). 3PO was administered intraperitoneally (i.p.) three times per week at the dose of 25 mg/kg. After six weeks, the mice received Cy5.5-labeled hyaluronan nanoparticles (HA-NPs) and fluorescent glucose analogue 2-NBDG 2 hours and 15 min before the sacrifice, respectively. The aortic accumulation efficacy of both probes was analyzed by IVIS imaging system. The aortic roots where sectioned for immunohistochemical evaluation.

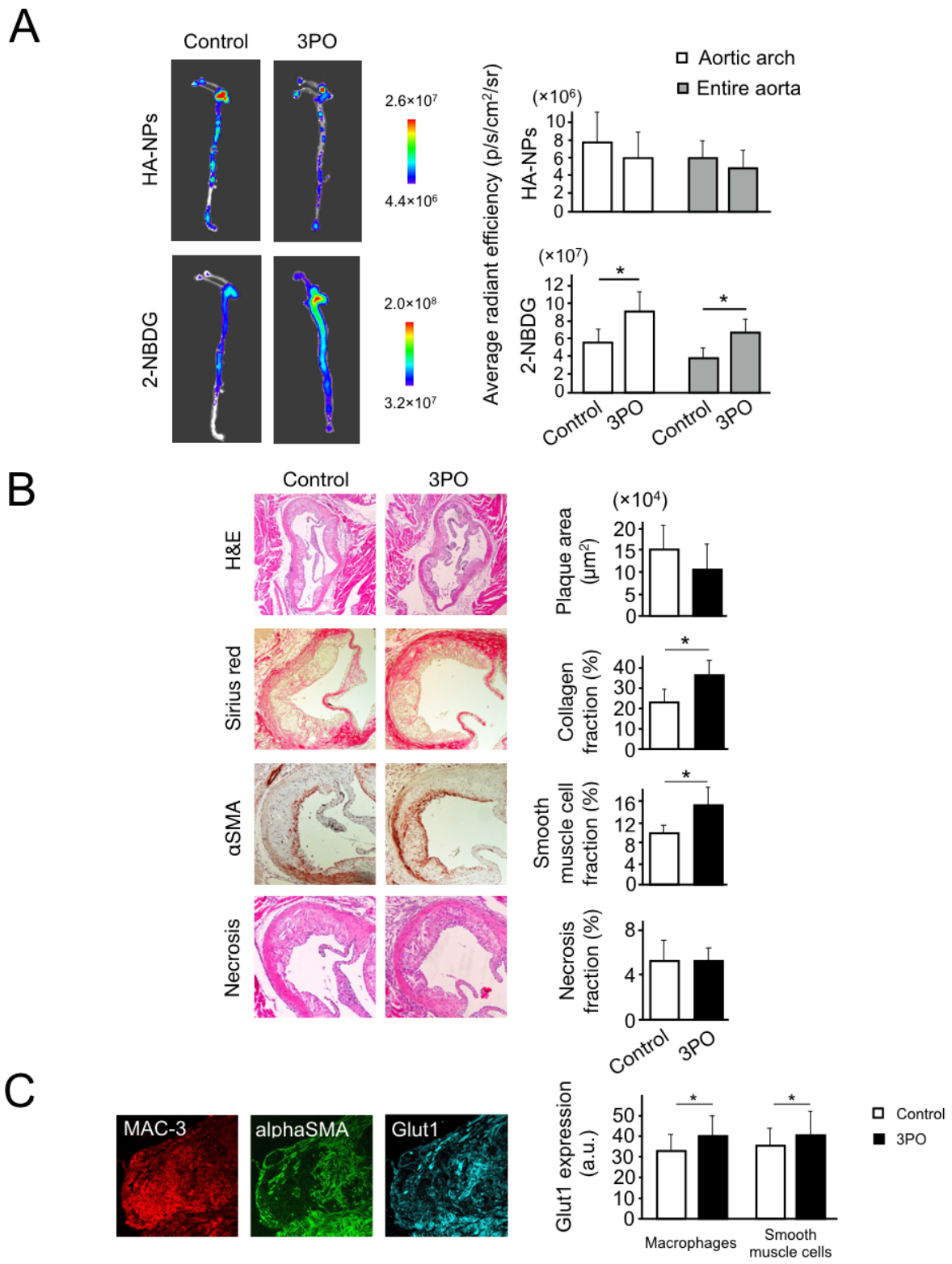

Figure S9 A) Representative IVIS images of aortas form non-treated mouse (control, left) and mice that underwent metabolic therapy (right). Upper panel displays Cy5.5-HA-NP signal, whereas the lower shows the fluorescence of 2-NBDG. The charts on the right show the average radiant efficiency generated by HA-NPs (upper) and 2-NBDG (lower) in aortic arches and full aortas. **B**) Histological data on the plaque size (top, hematoxylin and eosin (H&E)-stained), collagen content (second panel from the top, sirius red-stained), smooth muscle cell content (α-smooth muscle actin (αSMA-stained, third panel) and necrosis fraction (H&E-stained, fourth panel) in aortic roots of control and 3PO-treated mice. **C**) In the left panel, images of aortic root plaque section showing MAC-3-stained macrophages (red, left), αSMA-stained smooth muscle cells (green, middle) and

Glut1 expression (cyan blue, right). In the left, the chart displays the mean Glut1 fluorescence intensity (arbitrary units) in plaque-associated macrophages and smooth muscle cells for the investigated study groups. In all charts, bars represent mean ± SD; white bars: control; black bars: metabolic therapy. Symbol "*" represents a significant difference at $p<0.05$. The statistical comparison was performed with a two-tailed unpaired Student's t-test.

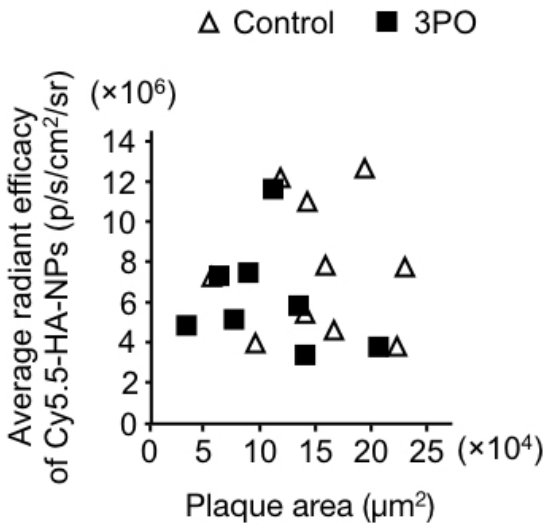

Figure S10 Relation between the average plaque area and average radiant efficacy generated by Cy5.5-HA-NPs signal in control (white triangles) and 3PO-treated mice (black squares).

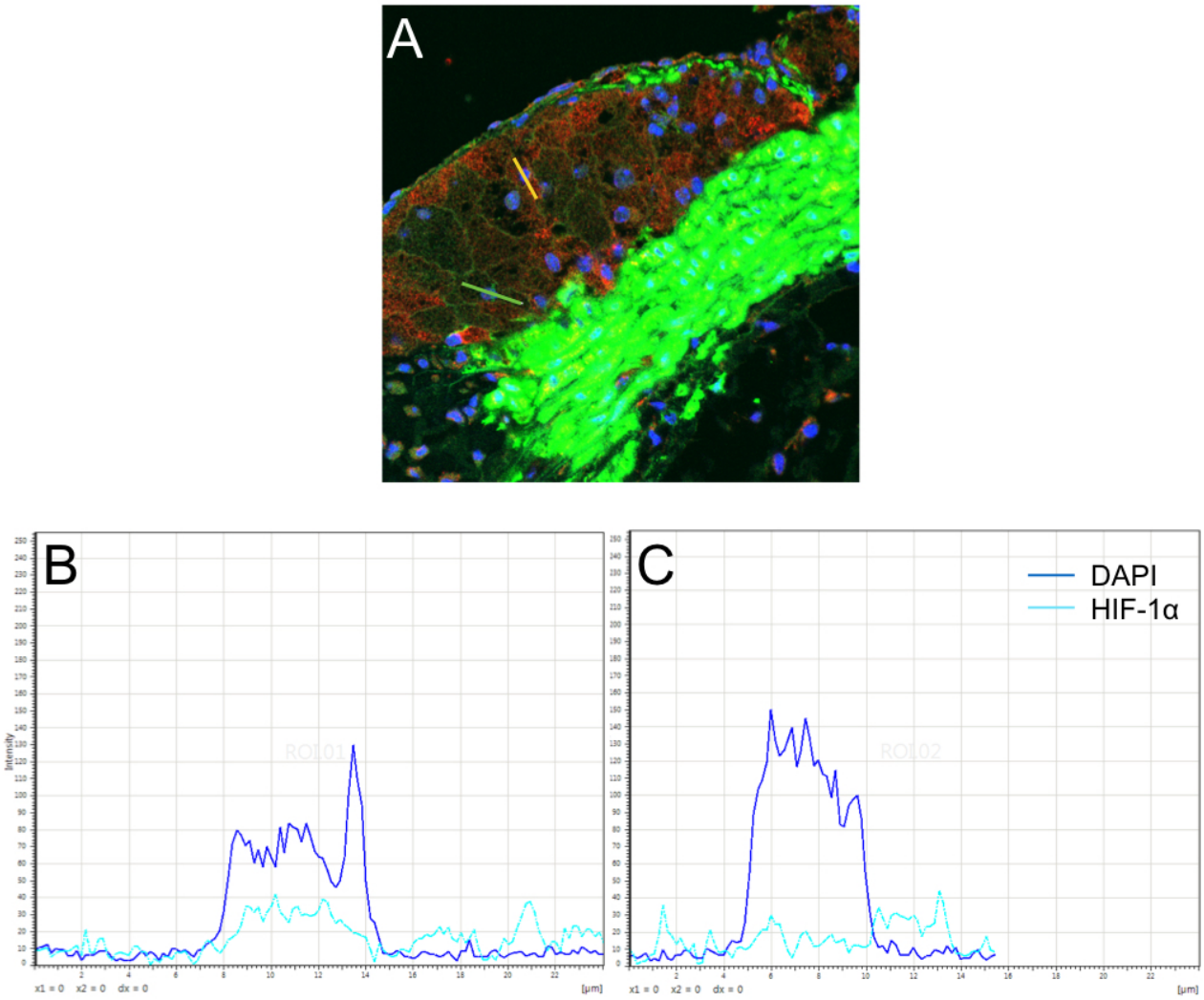

Figure S11 A) Representative plaque section, in which MAC3-stained macrophages and αSMA-stained-smooth muscle cells are shown in red and green, respectively. Nuclei were stained with DAPI (blue). Green and yellow line drawn through the cytoplasm and nucleus of two plaque-associated macrophages represent regions of interest, which were used to determine the nuclear translocation of HIF-1α. The corresponding histograms of Alexa Fluor 647-HIF-1α (cyan blue) and DAPI (dark blue) fluorescence intensity are displayed in **B**) and **C**). **B**) was considered as positive for nuclear HIF-1α, as deduced from HIF-1α signal intensity rise, colocalizing with DAPI signal. In contrast, **C**) was considered as negative since HIF-1α signal oscillated around the same level throughout the cell.

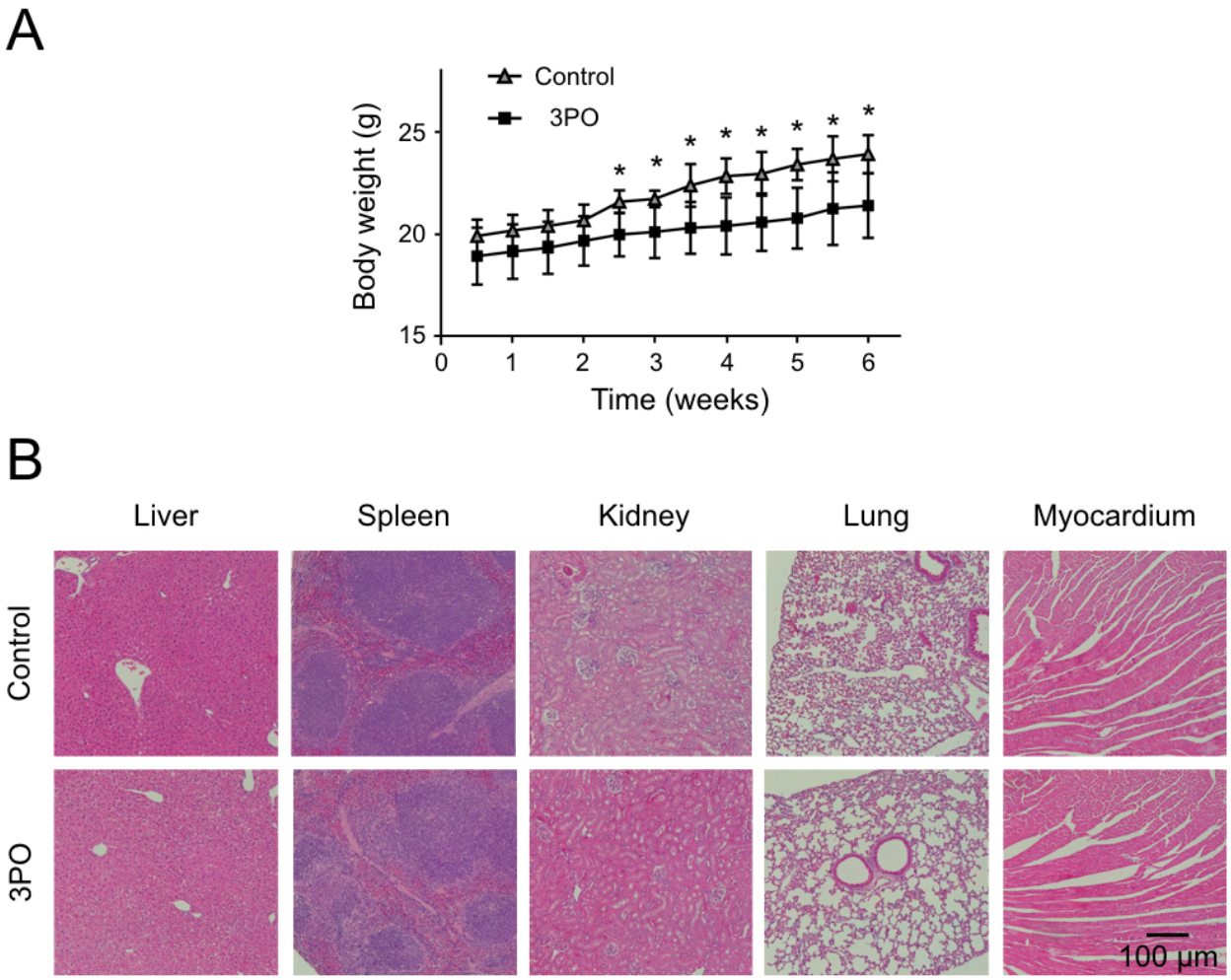

Figure S12 A) Weight-time curves of Control (gray triangles; n = 10) and 3PO-treated (black squares; n = 9) mice. "*" represents a significant difference at $p<0.05$. The group comparison was performed with a two-tailed unpaired Student's t-test at each study time point. **B**) Representative microscopy images of H&E stained sections of different organs from Control and 3PO-treated mice.

Table S1. Effects of 3PO therapy on hematological and metabolic blood parameters

	Control	Vehicle	3PO	P-value
Hemoglobin (mmol/L)	8.33 ± 0.25	8.40 ± 0.18	7.95 ± 0.87	ns
Hematocrit (L/L)	0.493 ± 0.017	0.490 ± 0.008	0.473 ± 0.057	ns
Erythrocytes (10^{12}/L)	9.34 ± 0.50	9.42 ± 0.21	8.99 ± 1.02	ns
RDW (%)	20.83 ± 0.86	20.25 ± 0.45	20.53 ± 1.35	ns
MCV (fL)	52.78 ± 1.24	52.10 ± 0.27	52.50 ± 0.56	ns
MCHC (mmol/L)	16.90 ± 0.08	17.10 ± 0.08	16.85 ± 0.19	ns
MCH (fmol)	0.893 ± 0.026	0.893 ± 0.005	0.885 ± 0.026	ns
Thrombocytes (10^9/L)	1149 ± 294	1367 ± 15	1300 ± 117	ns
Leukocytes (10^9/L)	5.05 ± 0.34	5.85 ± 0.86	5.50 ± 1.31	ns
Monocytes (% of CD45+ cells)	13.43 ± 3.51	10.87 ± 1.07	11.23 ± 1.14	ns
Ly6C high monocytes (% of monocytes)	21.00 ± 4.54	19.13 ± 4.28	22.63 ± 4.71	ns
Ly6C low monocytes (% of monocytes)	32.73 ± 1.34	34.43 ± 4.28	32.95 ± 2.00	ns
Neutrophils (% of CD45+ cells)	11.73 ± 1.98	17.00 ± 1.13	20.90 ± 7.48	ns
Eosinophils (% of CD45+ cells)	3.62 ± 0.69	2.25 ± 1.06	2.59 ± 0.80	ns
B-cells (% of CD45+ cells)	36.15 ± 2.92	43.23 ± 3.23	38.95 ± 5.83	ns
T-cells (% of CD45+ cells)	29.90 ± 4.62	24.47 ± 2.24	22.50 ± 4.68	Control vs 3PO: 0.025
CD4+ T-cells (% of T-cells)	50.84 ± 4.29	49.77 ± 1.40	50.24 ± 1.42	ns
CD8+ T-cells (% of T-cells)	41.43 ± 3.99	44.13 ± 0.72	44.40 ± 0.88	ns
AST (ng/mL)	127.5 ± 10.2	121.2 ± 2.5	116.1 ± 11.1	ns
ALT (ng/mL)	62.1 ± 12.7	62.3 ± 6.0	61.6 ± 8.0	ns
Albumin (mg/mL)	17.87 ± 0.71	17.40 ± 0.58	17.15 ± 0.93	ns
Cholesterol (mg/dL)	93.02 ± 3.26	96.10 ± 4.83	90.71 ± 4.82	ns
Triglycerides (mg/dL)	132.25 ± 21.11	163.52 ± 9.12	133.33 ± 11.86	Control vs Vehicle: 0.039 Vehicle vs 3PO: 0.045
Glucose (mmol/L)	9.60 ± 1.50	8.45 ± 0.45	8.73 ± 0.69	ns

Note: RDW: Red blood cell distribution width; MCV: Mean Corpuscular Volume; MCHC: Mean Corpuscular Hemoglobin Concentration; MCH: Mean Corpuscular Hemoglobin; AST: Aspartate transaminase; ALT: Alanine aminotransferase; Vehicle: dimethyl sulfoxide (DMSO); ns: non-significant; group size: n = 4; data were analyzed with one-way ANOVA and Turkey's post-hoc test

Ad. Methods

Cell culture

Primary human umbilical vein endothelial cells (HUVEC), pooled from five different donors, were purchased from Lonza (Basel, Switzerland) and cultured at 5% CO_2 and 37˚C in EBM-2 medium, supplemented with growth factors, 2% fetal calf serum, ascorbic acid, heparin, hydrocortisone (Promocell; Heidelberg, Germany) and antibiotics. Passaging of the cells was performed by trypsin digestion.

Human monocyte-derived macrophages (HMDM) were cultured from monocytes that were isolated from human buffy coats (Sanquin, Amsterdam, The Netherlands). Buffy coats were transferred to a T75 flask and diluted with HBSS (Gibco, ThermoFisher Scientific), containing 2% FCS, to a total volume of 100 mL. To isolate peripheral blood mononuclear cells (PBMC), 25 mL of diluted blood solution was carefully placed on top of 15 mL of lymphoprep (Axis-Shield; Dundee, United Kingdom) in 50 mL tubes. The samples were centrifuged for 30 min at 1000g, after which the white interface layer was collected and transferred to a new 50 mL tube. After an addition of 50 mL of HBSS containing 2% FCS, the samples were centrifuged for 7 min at 600g. The isolated PBMC pellet was collected and resuspended in IMDM medium (Gibco, ThermoFisher Scientific) supplemented with 1% FCS, at a concentration of 50 x 10^6 cells/mL.

To isolate the monocyte fraction from the PBMCs, 3 mL of cell suspension was placed on top of 10 mL of hyper-osmotic Percoll solution (48.5% Percoll (GE healthcare; Chicago, United States), 41% sterile water, 1.5 M NaCl solution) and centrifuged for 15 min at 580g. The white interface and upper layer were collected and IMDM containing 1% FCS was added. Subsequently, the cells were centrifuged for 7 min at 600g and the pellet was resuspended in 3 mL IMDM containing 1% FCS. The samples were placed on top of 10 mL of iso-osmotic Percoll solution (48.5% Percoll, 41.5% sterile water, 10% 1.6M NaCl solution) and centrifuged for 15 min at 580 g. The monocyte

pellet was collected and resuspended in IMDM containing 1% FCS. The concentration of cells was determined using a CASY cell counter (Innovatis, Roche)

The cells were seeded in tissue culture 96 wells plates (Greiner; Kremsmünster, Austria) at a density of 1 x 10^5 cells per well. Cells were allowed to attach for 2 h followed by medium replacement with 100 μL IMDM containing 10% FCS and 50 ng/mL M-CSF per well. Macrophages were allowed to differentiate for the following 6 days at 5% CO_2 and 37˚C. On day 3, the culture medium was refreshed.

Systemic effects of 3PO therapy

Eight weeks-old C57BL/6 mice (Janvier Labs, Le Genest-Saint-Isle, France) received either no treatment (Control) or three times per week intraperitoneal injections of either DMSO (Vehicle, 10% solution in 0.9% Saline) or 3PO (Sigma Aldrich; 25 mg/kg). After three weeks, the blood glucose level was determined in the blood from the tail tip by using a glucometer (Contour Next, Bayer, Leverkusen, Germany). The mice were sacrificed by CO_2 overdose and blood was sampled by a cardiac puncture, and mixed with 20 μL of 0.5M EDTA, used as an anti-coagulant. Hematological analysis of whole blood was performed at the Laboratory of Clinical Chemistry, Amsterdam University Medical Center. Blood plasma was used for the measurements of aspartate transaminase (AST ELISA kit, Biomatik, Cambridge, Canada), alanine aminotransferase (ALT ELISA kit, Biomatik), albumin (BCG Albumin Assay kit, Sigma Aldrich), cholesterol (CHOD-PAP method, Biolabo, Maizy, France) and triglycerides (GPO method, Biolabo). Blood immune cell composition was determined by flow cytometry. First, red blood cells were removed using hypotonic lysis buffer (0.15M NH4Cl, 10mM NaHCO3, 1mM EDTA). Subsequently, cells were incubated for 15 min with anti CD16/32 antibody for prevent fc-receptor binding (eBioscience, San Diego, USA). Myeloid cells were stained using anti CD45 (Biolegend, 30-F11, APC-Cy7), CD11b (eBioscience, M1/70, FITC), Siglec-F (BD Pharmingen, E50-2440, PE), Ly6G (BD Pharmingen, 1A8, PerCP-Cy5.5), CD11c (eBioscience, N418, PE-Cy7) and Ly6C (Biorad, ER-MP20, Alexa Fluor 647) antibodies. Lymphoid cells were stained using anti CD45 (Biolegend, 30-F11, APC-

Cy7), CD3 (eBioscience, 145-2C11, FITC), CD8 (eBioscience, 53-6.7, PE), CD19 (eBioscience, 1D3, PerCP-Cy5.5) and CD4 (eBioscience, GK1.5, APC) antibodies. For histological analysis tissue samples of all major organs were fixed with 4% PFA overnight, after which they were dehydrated and embedded in paraffin. Subsequently, the samples were cut in 4 μm sections and stained with hematoxylin and eosin. The stained sections were analyzed by a pathologist for any abnormalities.